

Model for reversible nanoparticle assembly in a polymer matrix

Andrew J. Rahedi

Department of Physics, Wesleyan University, Middletown, Connecticut 06459, USA

Jack F. Douglas

Polymer Division, National Institute of Standards and Technology, Gaithersburg, Maryland 20899, USA

Francis W. Starr^{a)}

Department of Physics, Wesleyan University, Middletown, Connecticut 06459, USA

(Received 10 April 2007; accepted 29 October 2007; published online 8 January 2008)

The clustering of nanoparticles (NPs) in solutions and polymer melts depends sensitively on the strength and directionality of the NP interactions involved, as well as the molecular geometry and interactions of the dispersing fluids. Since clustering can strongly influence the properties of polymer-NP materials, we aim to better elucidate the mechanism of reversible self-assembly of highly symmetric NPs into clusters under equilibrium conditions. Our results are based on molecular dynamics simulations of icosahedral NP with a long-ranged interaction intended to mimic the polymer-mediated interactions of a polymer-melt matrix. To distinguish effects of polymer-mediated interactions from bare NP interactions, we compare the NP assembly in our coarse-grained model to the case where the NP interactions are purely short ranged. For the “control” case of NPs with short-ranged interactions and no polymer matrix, we find that the particles exhibit ordinary phase separation. By incorporating physically plausible long-ranged interactions, we suppress phase separation and qualitatively reproduce the thermally reversible cluster formation found previously in computations for NPs with short-ranged interactions in an explicit polymer-melt matrix. We further characterize the assembly process by evaluating the cluster properties and the location of the self-assembly transition. Our findings are consistent with a theoretical model for equilibrium clustering when the particle association is subject to a constraint. In particular, the density dependence of the average cluster mass exhibits a linear concentration dependence, in contrast to the square root dependence found in freely associating systems. The coarse-grained model we use to simulate NP in a polymer matrix shares many features of potentials used to model colloidal systems. The model should be practically valuable for exploring factors that control the dispersion of NP in polymer matrices where explicit simulation of the polymer matrix is too time consuming. © 2008 American Institute of Physics. [DOI: [10.1063/1.2815809](https://doi.org/10.1063/1.2815809)]

I. INTRODUCTION

The addition of nanoparticle (NP) fillers to polymeric materials to form polymer nanocomposites often leads to greatly improved material properties. This has led to much excitement about the possible applications of these nanoparticles in many materials science applications.^{1–7} Though the quantitative understanding of the mechanisms behind these property improvements is still developing, it is well accepted that the surface area of NP in contact with the polymer matrix plays a pivotal role.² Moreover, the amount of NP surface area in contact with polymers depends on NP dispersion, and thus the problem of ensuring a stable NP dispersion has been a preoccupation with these materials.⁸

Computer simulations have been a useful tool for exploring the effect of various thermodynamic factors on NP dispersion and the properties of the resulting nanocomposite materials. Pryamitsyn and Ganesan have provided a recent review of theoretical efforts and their relation to experimental studies.⁹ The present paper describes computer simula-

tions of the self-assembly of nanoparticles into equilibrium clusters. Our results emphasize the role played by long-ranged polymeric interactions and the identification of the appropriate theoretical description of the underlying assembly process.^{10–13} The mechanism of cluster assembly is particularly relevant to polymer-NP composites, but has potential relevance for many fields, such as biological systems where molecular assembly often occurs in the “crowded” intracellular and extracellular environments.^{14,15}

Our study builds upon the observations made in an earlier study¹⁶ on the factors controlling NP dispersion in polymer melts. From Ref. 16 it was found that the NP underwent a thermally reversible transition to a clustered state upon cooling, in lieu of ordinary phase separation from the polymer matrix. The clustering had characteristics similar to those of equilibrium polymerization^{10–13,17,18} and micelle formation.^{19,20} Such assembly without the intervention of phase separation is recognized to occur when there are highly directional interactions that limit the coordination number and that inhibit the formation of close-packed clusters.²¹ However, such strongly directional interactions were *not* present for the icosahedral NP studied in Ref. 16;

^{a)}Electronic mail: fstarr@wesleyan.edu.

thus, the emergence of such equilibrium clustering without phase separation was somewhat surprising. In Ref. 16 it was hypothesized that the lack of phase separation might be a result of the fact that the range of the attraction of the NP was rather small compared to their diameter, similar to colloidal systems.²² If this is the origin of clustering in the nanocomposite, such clustering without intervening phase separation should also be apparent even if the NPs are not embedded in a polymer matrix. This is the basis of the first part of our work: We examine the phase behavior of a system of NP identical to those used in Ref. 16, but in the *absence* of the polymer matrix. Since we find that the particles in the absence of a polymer solvent phase separate rather than form thermally reversible clusters, our results indicate that there must be some other explanation for the clustering in the nanocomposite system.

An essential clue to understand the clustering of NP in a polymer matrix was provided by simulations of colloidal particles having a short-ranged attraction and a weak, long-ranged *repulsive* interaction potential.^{23–25} Sciortino *et al.* found a surprising result that particles with such isotropic interactions cluster in a similar fashion to particles with directional interactions.²³ In the present work, we argue that long-ranged interactions between NPs can arise from the polymeric matrix. In particular, we find that the thermally reversible NP clustering in a polymer matrix observed in Ref. 16 can be understood as a result of an effective long-ranged repulsive interaction between the NPs. From the perspective of characterizing nanoparticle dispersion in polymer melts, this finding is particularly relevant, as it suggests that a significant change in experimental protocol is needed to quantify nanoparticle clustering arising from dynamic association. Additionally, we compare our results with theoretical models of cluster formation at equilibrium to better understand the nature of this clustering transition.

The model we develop to address NP clustering in polymer melts involves coarse graining the polymer degrees of freedom to explore other aspects of NP clustering that would not be practical to simulate in a model that explicitly includes the polymeric component. We should be clear that our approach differs from that of a potential of mean force (PMF) approach. In the PMF approach, the aim is to derive a two-body potential directly from correlations between pairs of particles that can only quantitatively reproduce the behavior of a given thermodynamic state point. The PMF approach is not adequate to capture many-body interactions that are known to promote clustering in colloidal mixtures and polymer solutions.²⁶ Moreover, it is known that these many-body effects are especially large when the particle size is comparable to the polymer size, i.e., nanoparticles.²⁶ At the present time, we are aware of no general strategy to systematically derive an effective potential that accounts for the nonlocal many-body effects of the polymer fluid.

As a result, we adopt a pragmatic approach based on plausible physical arguments about the expected form of the effective potential involved that will effectively mimic the explicit polymer-nanocomposite system over a range of thermodynamic conditions. We check the consistency of this proposed potential by comparison with previous simulations

where the polymer molecules are explicitly incorporated.¹⁶ This semiempirical approach is in the spirit of recent modeling efforts to capture water mediated interactions by introducing effective polymer potentials.^{27,28} In both cases, these approximations are motivated by the desire to reduce the computational problem to manageable proportions.

The manuscript is organized as follows. In Sec. II we describe the key details of the model and simulation protocol. Section III describes the results of the NP with only short-ranged interactions. Section IV discussed the modification to the model to mimic polymeric interactions, the resulting assembly properties, and the relationship of our findings to recent theoretical models for particle clustering. This is followed by a brief conclusion to summarize our findings.

II. MODEL AND SIMULATIONS

We perform molecular dynamics simulations of 200 icosahedral NP with a constant number of particles N , constant volume V , and constant temperature T (NVT). Each NP contains 13 particles—12 of which are located at the vertices of an icosahedron and another at the center of the icosahedron, as described in Ref. 16. Hence the total number of force sites is 2600. In the simplest case, all particles interact via a 12-6 force-shifted Lennard-Jones (LJ) potential,^{29,30}

$$U_{\text{LJ}}^{\text{sf}}(r_{ij}) = \begin{cases} U_{\text{LJ}}(r_{ij}) - U_{\text{LJ}}(r_c) - \left[\frac{dU_{\text{LJ}}(r_c)}{dr_{ij}} \right] (r_{ij} - r_c), & r_{ij} \leq r_c \\ 0, & r_{ij} > r_c, \end{cases} \quad (1)$$

where U_{LJ} is the standard LJ potential, and we use “reduced units” such that the LJ energy parameter $\epsilon=1$ and the length parameter $\sigma=1$, and the particle mass $m=1$. The only difference in the potential from Ref. 16 is that in Ref. 16 they used $\epsilon=2$, shifting by a factor of 2 the units of temperature. In these reduced units, time is in units of $\sigma\sqrt{m/\epsilon}$, temperature is in units ϵ/k_B , where k_B is the Boltzmann constant, and pressure is in units of ϵ/σ^3 .

To maintain the icosahedral shape of a NP, adjacent particles within a NP interact via a harmonic spring potential,

$$U_{\text{harm}}(r) = \kappa \frac{r_0^2}{2} \left(\frac{r}{r_0} - 1 \right)^2, \quad (2)$$

where $\kappa=90$ and r_0 is the preferred bond length. For particles at the vertices that are directly connected along an edge, r_0 is given by the distance of the minimum of $U_{\text{LJ}}^{\text{sf}}$. The center particle is bonded to all the vertex particles to provide stability to the NP. The preferred bond length between the core and vertex particles is $r_0^c = 1/4(10+2\sqrt{5})^{1/2}r_0$, which is the radius of sphere that circumscribes the vertices of an icosahedron with edge length r_0 . In some cases, we will introduce size dispersity to avoid crystallization, or we will add a long-ranged interaction. We will discuss these modifications as they become relevant.

We integrate the equations of motions using the velocity Verlet version of the reversible reference system propagator algorithm (rRESPA).³¹ We separate our forces into bonded

(fast) and nonbonded (slow) components, where one update of the nonbonded forces occurs for every three updates of the bonded force. We use a time step $\delta t = 0.002$ for bond forces. We use the Nose-Hoover thermostat^{29,30} to deterministically control the temperature. The “mass” of the thermostat $Q = 6NT/\omega^2$, where $\omega = 234.09$ is the frequency of the cubic LJ lattice.³²

III. PURE NANOPARTICLES WITH ONLY SHORT-RANGE ATTRACTION

In spite of the highly symmetric form of the NP studied in Ref. 16, the NPs were found to reversibly cluster rather than phase separate when embedded in a polymer melt.³³ Of course, the discrete force sites imply that the potential is not spherically symmetric, but for systems with ≈ 12 sticky spots in three dimensions, recent work suggests that the phase boundaries are nearly coincident with those of the corresponding spherically symmetric potential.^{21,34} However, if the range of attraction δ relative to the size σ of the NP is small ($\delta/\sigma \lesssim 0.3$), the critical temperature for phase separation can be greatly reduced also for spherically symmetric potentials, as in colloidal systems.²² The size σ can be estimated from a pair distribution function, but the estimation of δ is less clear. Depending on the estimate for δ , the ratio δ/σ is in the range $0.25 \lesssim \delta/\sigma \lesssim 0.5$, so that the importance of these size ratio effects on phase separation is uncertain in our calculations.

Thus, our first objective is to quantify the effect of the patchiness and range of the potential on phase separation, so that we may separate these effects from polymeric interactions when the NPs are embedded in a polymer matrix. We simulate pure NPs over a range $1.55 \leq T \leq 1.9$ (in intervals $\Delta T = 0.05$), with many densities for each T , and determine the mean pressure P to construct the P - V phase diagram shown in Fig. 1(a). The presence of a “loop” in the isotherms—a region of positive slope—is indicative of the presence of a first order phase transition. Figure 2 shows snapshots of our system at state points corresponding to the various phases of our system. We attribute the negative pressures that we observe at $T \lesssim 1.7$ to the ability of the network of NPs to sustain a tension in metastable states.³⁵ To obtain smooth estimates of the P - V isotherms, we fit the data from the simulations along isochores to a fourth order polynomial, and the data along isotherms to a fifth order polynomial. The resulting combined expression allows us to estimate P - V data anywhere in the region simulated.

We use these fits to estimate the coexistence and spinodal lines of the transition, which we determine using the Maxwell construction (i.e., the equal area/equal free energy condition). We also use the information from the P - V phase diagram to construct the more common P - T phase diagram [Fig. 1(b)]. Figure 1 shows that the critical point occurs at $T_c \approx 1.8$, $V_c/N \approx 38.2$, and $P_c \approx 0.013$. For comparison, a simple LJ system with interactions truncated at the same distance, $T_c = 1.1876 \pm 0.0003$,³⁶ considerably below the T_c for our system. This can be understood from the fact that there are 13 force sites in a single nanoparticle, and thus the magnitude of attraction between NP is significantly greater.

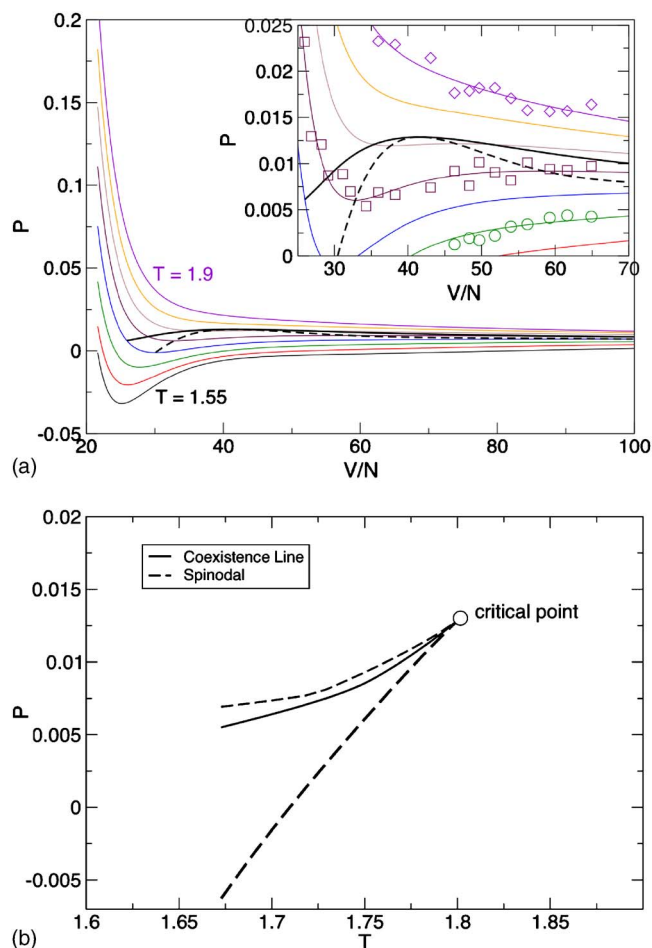


FIG. 1. (Color online) Equation of state for coarse-grained nanoparticle dispersion model. (a) The P - V phase diagram for pure NPs. The inset is a blowup of the region close to the critical point to emphasize the shapes of the coexistence (heavy solid black line) and spinodal (heavy dashed black line) lines. We show sample data for P (symbols) that were used to determine the isotherms (in solid lines), and the coexistence (red dashed line) and spinodal lines (dashed blue line). See text for the fitting procedure used to obtain these lines. (b) P - T phase diagram showing the coexistence line (solid line) and the spinodal line (dashed line), from which we get the critical point $T_c \approx 3.60$, $V/N_c \approx 2.94$, and $P_c \approx 0.026$.

Based on this, one might expect the value of T_c we observe to be much higher than that for the simple LJ system, but the relatively small δ/σ ratio serves to reduce T_c , and hence the overall change in the critical temperature is not nearly so substantial. To compare directly with the simulations of the same particles in a polymer matrix,¹⁶ where no phase separation was observed for $T > 1$, the value of T_c must be doubled, since in that work we chose $\epsilon = 2$ for the interactions between the nanoparticles. In the current dimensionless variables, the phase separation in the prior simulation was suppressed to at least $T < 0.5$, a temperature well below where we find phase separation. Evidently, there is some aspect of the polymer-nanoparticle dispersion that is responsible for the suppression of phase separation. The obvious possibility is that many-body interactions generated by chain connectivity alter the nature of the thermodynamic transition governing the particle dispersion, changing this process from phase separation to self-assembly where the solvent is replaced by a polymeric one.

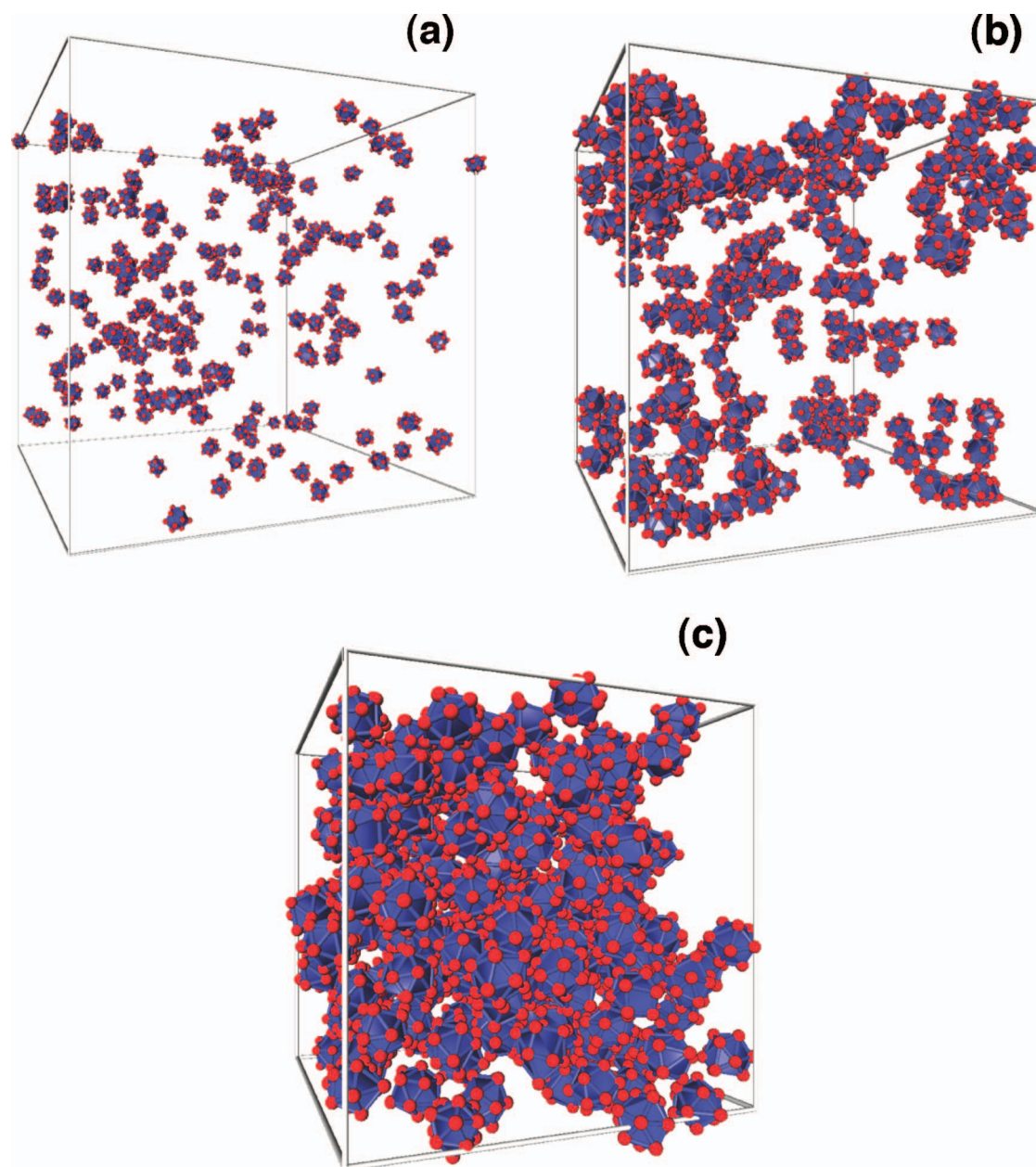


FIG. 2. (Color) Snapshots illustrating the particle dispersion under different thermodynamic conditions: (a) a gas phase system at $T=3.3$, $V/N=50.0$; (b) a gas-liquid phase system at $T=3.3$, $V/N=10.0$; and (c) a liquid phase system at $T=3.3$, $V/N=2.5$.

IV. MIMICKING POLYMERIC EFFECTS ON NANOPARTICLE BEHAVIOR

A. Effective polymeric interactions

Since the phase separation observed in the previous section is absent in the corresponding nanocomposite system,¹⁶ we must modify the potential of the pure NP system to mimic the behavior of the nanocomposite, as well as investigate the general properties of assembly. First, we know that our pseudopotential should at least retain the explicit short-ranged LJ interaction between NP. At a coarse-grained level, we can view the polymer chains as soft segmental clouds represented by “soft spheres,”³⁷ which naturally leads to a mean field model where the long-ranged contribution to the effective potential is identified with the average segmental density of a polymer chain. Along similar lines, Hooper and

Schweizer³⁸ describe polymers as “cushions” that provide a soft repulsion between NP. Hence we need to include a second term in the potential that involves a weak, long-ranged repulsion. A symmetric potential should be adequate since Refs. 39–43 argue that the secondary fluctuations are not necessary to reproduce NP interactions in the polymer matrix.

The question is as follows: What form should we choose for the long-ranged repulsion? Recent theoretical work⁴⁴ indicates that chain connectivity in polymer melts can generate Casimir-like interactions between particles in polymer melts where segmental density fluctuations induce interactions at long distance that are repulsive, rather than attractive, as in ordinary Casimir interactions where vacuum fluctuations are involved. In this case, the long-ranged repulsion has an exponential decay that is on the scale of the chain radius of

gyration. A similar exponential weak repulsion arises from screening effects in semidilute polymer solutions,⁴⁵ where the repulsions can be modeled by a Yukawa potential,

$$U_Y(r) = A \frac{\exp(-r/\xi)}{(r/\xi)}, \quad (3)$$

where A is the overall strength of the potential, and ξ is the parameter that determines its range. Such a potential fulfills the physical criteria described above for a polymer-NP mixture. Since the segmental density of the polymer should be responsible for the repulsive potential, the parameter ξ must have a scale somewhere between a segment size and the radius of gyration of a chain. When the Yukawa interaction is combined with the direct LJ interactions, the overall potential is dominated by LJ terms at short and intermediate distances, and the effect of the Yukawa potential contributes to the particle interactions at large distances.

The relevance of the Yukawa potential for polymer-induced nanoparticle interactions potential is further supported by Refs. 23–25. In those works, it was shown that particles with an attractive short-ranged potential in combination with a long-ranged repulsive Yukawa interaction indeed undergo self-assembly rather than phase separation for certain choices of the potential parameters. These findings give us confidence that our pseudopotential may contain enough of the essential physics of polymer melts to understand the former nanoparticle self-assembly observations in polymer melts.¹⁶

Given the long-range nature of repulsive part of potential, it is natural and computationally expedient to further approximate the collective effect of all the individual Yukawa potentials on each atomic site of the nanoparticle by a single effective Yukawa potential U_Y^c acting between the centers of nanoparticles. The coupling strength of this potential is taken to be equal to the number of force sites in the nanoparticle times that of an individual atom U_Y , so that effective long-ranged potential interaction has an equal contribution from each force site of the nanoparticle. This is reasonable approximation since the separations at which the Yukawa potential plays an important role are large compared to the distance between the NP center and vertices. This approximation reduces dramatically the computational time needed, while preserving essential aspects of the more detailed potential.

Since our approach to arrive at the Yukawa potential is based on physical arguments, rather than direct approaches such as the PMF, the appropriate parameters of the potential are not immediately clear. The primary concern is that the choice for A and ξ should reproduce the essential physics that is known about nanoparticle clustering in the polymer matrix—and that ξ is in the range between the segmental size and chain radius of gyration. Based on the studies of Mossa *et al.*²⁴ and preliminary test simulations, we found that if $A = 0.15$ and $\xi = 2$ this yields significant particle clustering, while strongly suppressing phase separation, and satisfies the size constraints on ξ . However, our preliminary calculations showed that the clusters formed by our icosahedral NP have a quasicrystalline structure. To generate amorphous clusters, we further introduce dispersity in the nanoparticle size,

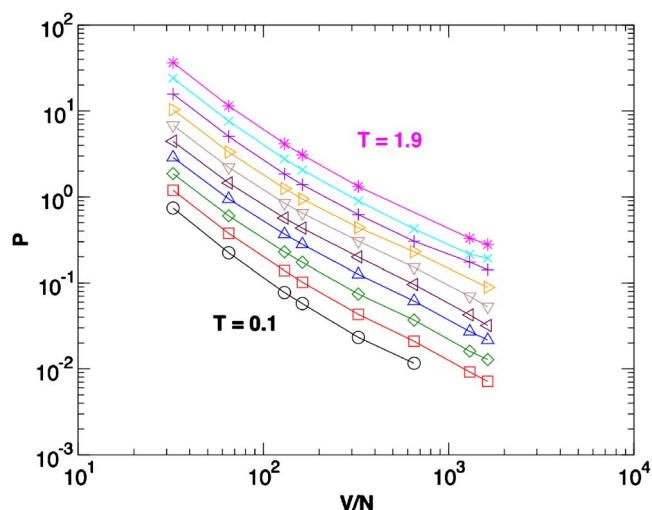


FIG. 3. (Color online) Isotherms of P vs V/N for the modified NP with the Yukawa potential. The lack of a “loop” indicates that the long-ranged repulsion suppresses phase separation down to at least $T < 0.1$. Each isotherm is separated by 0.2 in temperature, and curves are progressively shifted by a factor of 1.5 on the pressure axis for clarity. The lines are intended as a guide for the eye.

thereby frustrating this ordering. (Alternatively, we could take ξ to be a variable among the NP.) For half of the NP, we reduce the overall NP size by 20% by assigning a force site of diameter $\sigma_{ss} = 0.8$, where the subscript ss denotes pairs of smaller force sites. We use a subscript ll , i.e., $\sigma_{ll} = 1$, for pairs with unchanged size, which we refer to as large. For the mixed interactions between small and large force sites we choose $\sigma_{ls} = 0.9$. In addition to changing the size of the force sites, we also decrease the bond lengths [see Eq. (2)] between small force sites by 20% so that the NPs with the smaller force sites are also overall smaller by 20% than the original NP. We find that an equal mixture of NP of these sizes suppresses the quasicrystalline structure of the clusters and yields the desired amorphous clusters. We simulate this modified potential over a range $0.008 \leq N/V \leq 0.4$ and $0.1 \leq T \leq 1.9$, and report the results in the following.

B. Basic thermodynamic and cluster properties

We first evaluate the pressure along isotherms to verify that adding the long-range interactions is effective in suppressing phase separation. The P - V plot of the system with Yukawa interactions in Fig. 3 does not exhibit a van der Waals loop (as found in Fig. 1) in the range of T and V investigated, and thus there is no apparent phase separation for $T \geq 0.1$. This temperature is well below T_c for the system with attraction only. Hence, as in the nanocomposite system of Ref. 16, phase separation is suppressed while significant equilibrium particle clustering can occur in its place. In this system, the particles cluster due to short-ranged attraction, but the cluster size is limited (and hence infinite phases cannot develop) by the long-range repulsion.^{23,24}

As discussed in the Introduction, Refs. 23 and 24 have shown that a combination of short-range attraction and repulsive Yukawa potentials can result in reversible equilibrium particle clustering. Here we expand on those calculations, and we particularly focus on calculating properties relevant

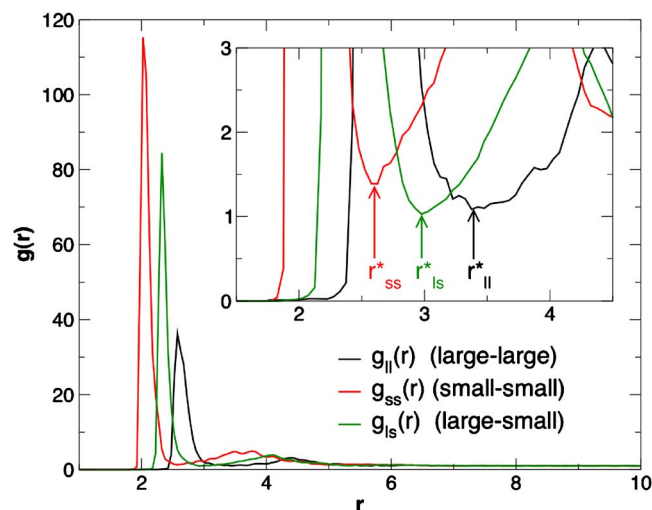


FIG. 4. (Color online) The pair distribution function $g(r)$ between the centers of NP. We separate $g(r)$ into the contributions between pairs of small or large NP, and also the cross correlations between small and large NPs. We define particles to be nearest neighbors if $r < r^*$, where r^* is the location of the minimum of $g(r)$. (Inset) An expanded view of $g(r)$ near r^* . The arrows show the locations of the r^* for the three possible pairs.

to nanoparticle clustering in polymer melts and to connecting the clustering behavior with an existing theoretical model for particle clustering.

We first quantify the assembly by defining clusters as collections of neighboring NP. We consider NPs to be nearest neighbors if their center atoms are within r^* , the distance of the first minimum in the center-center NP pair distribution function $g(r)$ (Fig. 4). Since our system is bidisperse, we have three values defining first neighbors for the three possible pairings of NP: $r_{II}^* = 3.44$, $r_{ss}^* = 2.58$, and $r_{ls}^* = 2.96$.

The overall amount of clustering can be characterized by calculating the fraction Φ of NPs that are in clusters, i.e.,

$$\Phi = \frac{1}{N} \sum_{\text{clusters}} n, \quad (4)$$

where n is the number of NPs in a cluster and N is the total number of NP in the system. This is analogous to the “extent of polymerization” discussed elsewhere.^{10–12} We plot Φ as a function of T in Fig. 5, which shows a crossover to a predominantly clustered state at low T , as found before for bare particles within a polymer matrix.¹⁶ The results in Fig. 5 establish that the NP assembly follows a classic pattern for self-assembling systems, not previously explored in Refs. 23 and 24.

To estimate the crossover temperature governing this self-assembly transition, previous works have often utilized the inflection point of $\Phi(T)$ to define this temperature.^{10–13,46,47} Unfortunately, our data are not sufficiently detailed to make an accurate estimation of the inflection point of Φ , and so we rely on an approximate method using the cluster mass that has been found to be useful.⁴⁷ The average cluster mass L is defined as

$$L = \langle n \rangle. \quad (5)$$

We plot L as function of T in Fig. 6(a), which shows that L increases as T decreases and, correspondingly, Φ increases.

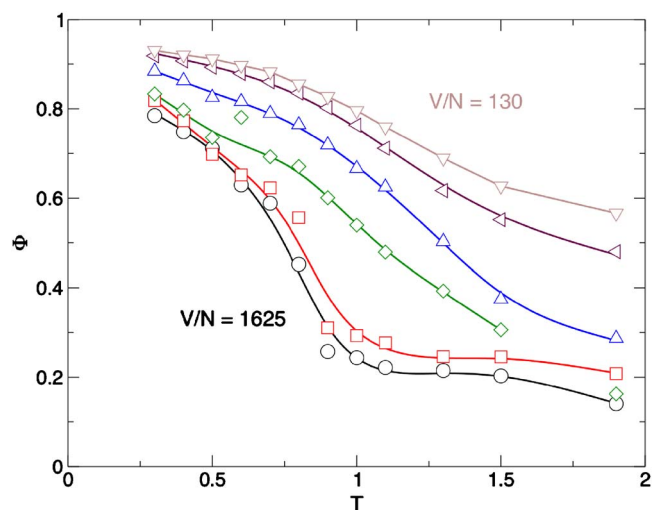


FIG. 5. (Color online) Fraction Φ of clustered NP as a function of T . At low T we observe that most NPs are in a clustered state. As we increase T , the system becomes dispersed, except for large density (low V/N) where clusters are unavoidable. The lines are only intended as a guide to the eye, and are the results of spline fits to the data.

These are the normal trends for a system exhibiting dynamic clustering at equilibrium.^{10–13} Investigating the clustering in a dipolar system, Van Workum and co-workers,^{47,48} found that L for a clustering dipolar fluid could be collapsed to a single master plot by scaling the temperature axis by the temperature where $L \approx 2$. Similar scaling has been found using the predictions of the Wertheim theory.^{49,50} The $L \approx 2$ condition seems to be a common property of thermally reversible associating particle systems exhibiting a broad particle clustering transition. Accordingly, we take $T^* \equiv T(L \approx 2)$ a definition for the self-assembly transition temperature.

We scale the T by T^* and find that we can collapse our L data to a master curve [Fig. 6(b)], consistent with an appropriate definition of the clustering transition temperature. Thus, the condition $L \approx 2$, i.e., the formation of dimers (on average), is indicative of a crossover from an unclustered to a clustered state. Moreover, the existence of a master curve

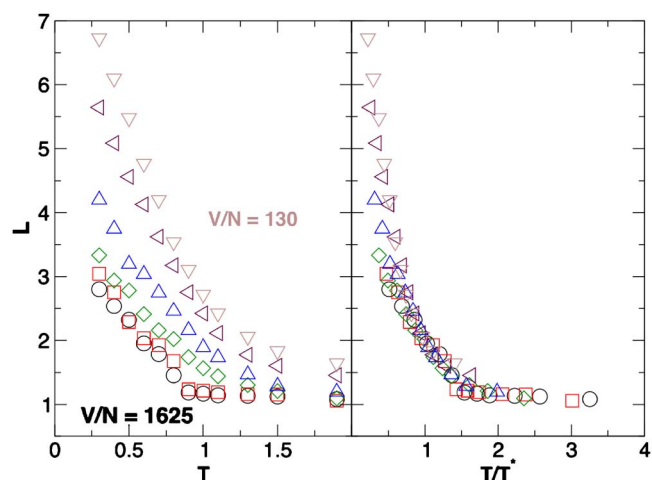


FIG. 6. (Color online) (a) Average cluster mass L as a function of T along isochores. (b) The same data with a reduced temperature scale, where T is normalized by $T^* \equiv T(L \approx 2)$, show that the data collapse to a single master curve.

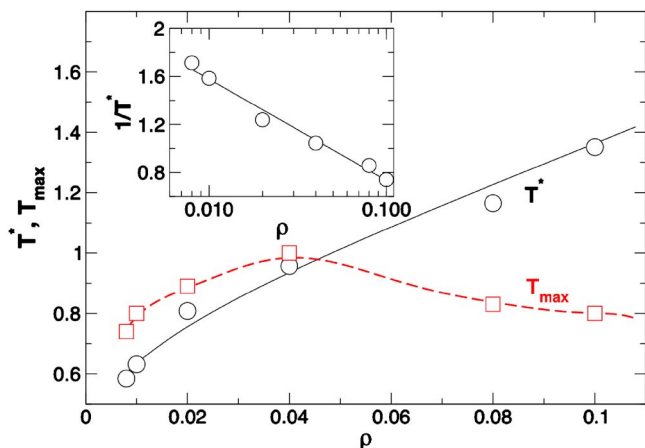


FIG. 7. (Color online) A comparison between the particle clustering transition temperatures T^* and T_{\max} estimated from L and c_v , respectively. The nonmonotonic behavior of T_{\max} suggests that c_v is not a good measure of the assembly transition temperature for this system. The inset shows that T^* conforms reasonably well to an Arrhenius relation, as expected from simple theoretical models of equilibrium particle assembly. The black line indicates the best fit of Eq. (7); the red dotted line is only a guide for the eye.

indicates that the T dependence of cluster mass is independent of the thermodynamic details. We can also scale our data for Φ by T^* , and we obtain an approximate collapse of the data, although the quality of the collapse is not as good as the reduction found for L . This type of reduction shows the potential for equation of state reasoning for organizing observations relating to cluster dispersion, analogous to the “corresponding states” descriptions of phase stability. We have also examined the distribution of cluster sizes $P(L)$ (not shown) which collapse to a master curve when scaled. We find that $P(L)$ has a power-law dependence on L , with an exponent in the range of 2.2–2.6. Such power-law dependence is consistent with branched polymers or percolation clusters.⁵¹ In contrast, the assembly of linear chain clusters leads to an exponential dependence of $P(L)$.

Previously, the specific heat c_v has been used as a measure to distinguish the crossover between dispersed and clustered states.^{10–12,16,52} Typically, both dispersed states and clustered states are relatively stable, and thus have relatively low energy fluctuations. Since c_v is a measure of such fluctuations, the crossover between clustered and dispersed states can be expected to be accompanied by a maximum in c_v . To check for the equivalence of this measure, we evaluate the specific heat,

$$c_v = \left(\frac{\partial u}{\partial T} \right)_v, \quad (6)$$

where u is the nonbonded (LJ) component of the potential energy per particle. We determine c_v from the derivatives of splines of $u(T)$. We find that for each density there is a weak maximum in c_v (not shown) at a temperature we call T_{\max} . This provides an estimate of the crossover to a clustered state based on a bulk thermodynamic property that we can compare with T^* .

We plot the density $\rho = N/V$ dependence T_{\max} and T^* in Fig. 7 to compare the crossover measured via these different approaches. We find that T^* has the expected dependence,

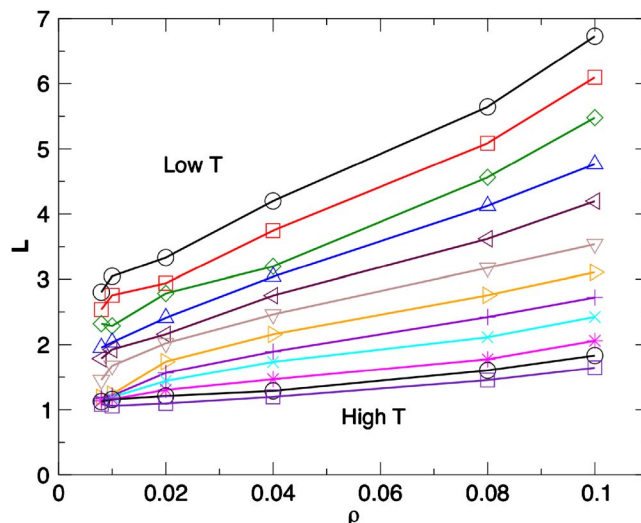


FIG. 8. (Color online) The average cluster mass L as a function of density ρ for various T . Note that $\rho \propto L$ for our system, similar to the behavior of wormlike micelles, colloidal fluids, protein suspensions, and dipolar fluids (Refs. 47, 54, and 55). The lines simply connect data points.

that is, T^* increases with ρ , since at larger density it will be easier to form clusters. The same is true for T_{\max} for $\rho \leq 0.04$; however, we find that T_{\max} decreases for $\rho > 0.04$, in contradiction to the expected monotonic behavior found for other associating fluids.^{10,11,16,52} This behavior suggests that the maximum in c_v is not necessarily a good indicator of the location of the clustering transition.

Frequently, the crossover T^* to an assembled state can be described by the Dainton-Ivin equation of equilibrium polymerization theory,⁵³ which is given by the simple “Arrhenius” form.^{10–12,16}

$$\rho \propto \exp(-E/k_B T^*), \quad (7)$$

where E is the enthalpy of association. We plot $1/T^*$ as function of ρ in the inset of Fig. 7 and just find such a relationship with $E=2.7$. This provides an estimate of the thermodynamic activation energy associated with the physical bonds formed between NP. Hence, we conclude that our system undergoes processes similar to associating systems generally.⁴⁶ When we combine the results of the masterplot in Fig. 6 and the Arrhenius property in Fig. 7, we conclude that T^* is of greater relevance than T_{\max} for analyzing clustering behavior in our system.

Lastly, we turn our attention to the ρ dependence of L , which has not been examined computationally in this class of associating fluids. It has been found that L scales as $L \propto \rho^{1/2}$ in many freely associating (FA) clustering systems.^{13,17,18,32} We might also expect that nanoparticles in our system are also freely associating, but Fig. 8 shows that L has an approximately linear ρ dependence. This observation has some precedence in previous experimental and computational studies. For example, a linear dependence has been observed in systems such as wormlike micelles⁵⁴ and the Stockmayer fluid,⁴⁷ where long-ranged interactions also play an important role. This variation has also recently been reported⁵⁵ for colloid and protein solutions, where matrix

mediated interactions and screened Coulomb interaction are plausibly present.

Dudowicz *et al.*¹³ found that linear concentration dependence of L is a generic phenomenon in equilibrium associating systems that are subject to constraints, thus limiting the assembly process. In particular, Dudowicz *et al.*¹³ demonstrated this effect in the context of equilibrium polymerization subject to the constraint of chemical initiation or thermal activation. For example, simply constraining the number of particles that are required before a cluster can form linearizes $L(\rho)$.⁵⁸ The results of Ref. 56 support these general arguments by showing that a change in $L(\rho)$ occurs with the introduction of a ring-formation constraint into a model of otherwise freely associating chains. The observation of a near linear dependence of $L(\rho)$ in the present model strongly suggests the existence of a constraint, but its specific form is not yet established. We suggest that the high functionality (number of contacts) of the particle associations may create a steric bottleneck in the assembly process, providing a candidate for this constraint. We also note that the introduction of constraints into the self-assembly process also tends to make the thermodynamic transition sharper (i.e., less rounded).^{12,57} Taking these constraints to extreme limits can make the self-assembly transition a true second-order phase transition.⁵⁸ This is an aspect of the assembly process that merits investigation in future work.

V. CONCLUSION

Recently, there has been much interest in understanding self-assembly from a more fundamental perspective due to the relevance of self-assembly for nanofabrication applications. There have also been many computational and experimental studies aimed at controlling nanoparticle dispersions because of the commercial potential of these materials. The present work touches on both of these basic fields. In particular, we find that a simple long-range interaction can be used to represent the polymeric effects that qualitatively alter the type of thermodynamic transition governing particle dispersion in the polymer matrix. In particular, the presence of the polymers changes the phase separation process into a thermally reversible self-assembly transition. Moreover, we find that this assembly is consistent with the theoretical description of association with constraints.¹³ This finding means that characterizing nanoparticle association in a polymer matrix is not just a problem of phase stability, but involves a significant change in experimental protocol to quantify nanoparticle interactions. Such solvent-induced effects are not limited to polymeric systems. For example, fullerene particles have been observed to form different types of clusters, depending on the solvent in which the fullerenes are dispersed.^{59,60} The solvent has also been found to play an important role in the supramolecular assembly of conjugated molecules into nanofibers.⁶¹ The interaction of nanoparticles with biological materials is an important situation where this effect arises. Hence, the general problem of how the medium in which such particles are placed generates effective interparticle interactions merits further investigation.

Given the complexity and time consuming nature of

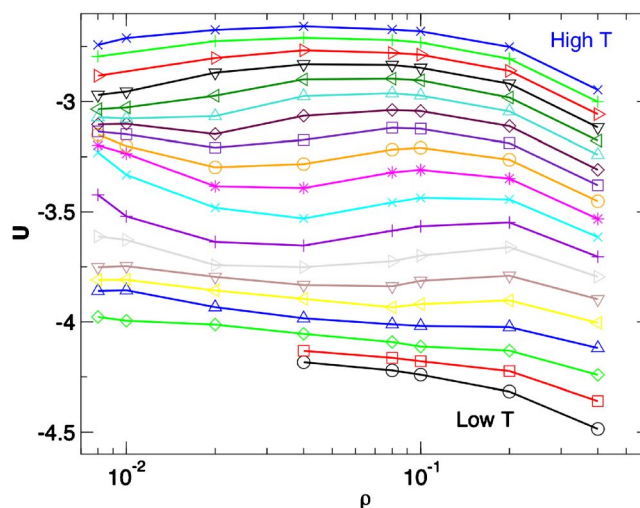


FIG. 9. (Color online) Potential energy as a function of density, showing a double-well structure in the potential energy. If there were phase separation, the free energy $F=K+U-TS$ would have a double-well dependence on density; thus the density dependence of the entropy must be responsible for the lack of phase separation. The lines simply linearly interpolate between points.

fully explicit molecular dynamics simulations of dispersions of NP in polymer matrices, it is very encouraging that some of the essential physics of NP association in a polymer melt can be recovered from a simple coarse-grained pseudopotential model. Moreover, our simple model of the interparticle interactions generated by the polymer fluid helps us understand the physical origin of the clustering transition that we observed previously.¹⁶ The existence of long-ranged effective interactions is expected to be a general feature of polymer melts, where the interactions are derived from long-ranged density correlations associated with chain connectivity.⁴⁵ Coarse-grained models of the effective nanoparticle interactions offer the potential to treat problems that are essentially impossible to treat by atomistic or even a bead-spring-like description of the polymer matrix.

ACKNOWLEDGMENTS

We thank S. V. Buldyrev for the code that generate the spinodal and coexistence lines shown in Fig. 1. We thank the NSF for support under Grant No. DMR-0427239.

APPENDIX: THE PHASE BOUNDARY “SHADOW”

For the system with Yukawa interactions, we do not find explicit phase separation, but we do find at least a precursor to separation in the potential energy of the system $U=U_{LJ}+U_Y$ (neglecting the contribution from the bonds, which is nearly constant). For a system where temperature and density are the control parameters, the appropriate free energy is the Helmholtz free energy $A=K+U-TS$, where K is the total kinetic energy, U is the total potential energy, and S is the entropy.⁶² Phase separation in such system results in a “double-well” shape of A as a function of ρ . Since we do not have information on S , we cannot plot A , but we can examine the contribution from U .

Figure 9 shows that a single-well structure appears in U

for $T \leq 1.5$ and $\rho \approx 0.04$. Additionally, when ρ is larger than that shown in Fig. 9, U must increase due to a short-ranged repulsion, and hence there will be a second well. Therefore, the contribution of U to A already has the characteristic shape for phase separation, but A must not have this shape, since no phase separation is present. Given that the contributions from K and S must be monotonically decreasing as the system cools, and assuming the behavior of U is unchanged, we would expect that A eventually does in fact develop a double-well structure, and hence there would be phase separation at sufficiently small T . In this sense, we say that phase separation is suppressed due to the entropic term.

- ¹G. Wypych, *Handbook of Fillers* (ChemTec, Toronto, 1999).
- ²R. A. Vaia and E. P. Giannelis, *MRS Bull.* **26**, 394 (2001).
- ³M. E. Mackay, T. T. Dao, A. Tuteja, D. L. Ho, B. Van Horn, H. Kim, and C. J. Hawker, *Nat. Mater.* **2**, 762 (2003).
- ⁴M. F. Mackay, A. Tuteja, P. M. Duxbury, C. J. Hawker, B. Van Horn, Z. Guan, G. Chen, and R. S. Krishnan, *Science* **311**, 1740 (2006).
- ⁵Y. Kojima, A. Usuki, M. Kawasumi, A. Okada, T. Kurauchi, and O. Kamigaito, *J. Mater. Sci.* **8**, 1185 (1993).
- ⁶F. W. Starr, T. B. Schröder, and S. C. Glotzer, *Phys. Rev. E* **64**, 021802 (2001); F. W. Starr, T. B. Schröder, and S. C. Glotzer, *Macromolecules* **35**, 4481 (2002).
- ⁷S. T. Knauert, J. F. Douglas, and F. W. Starr, *J. Polym. Sci., Part B: Polym. Phys.* **45**, 1882 (2007).
- ⁸K. Yano, A. Usuki, A. Okada, T. Kurauchi, and O. Kamigaito, *J. Polym. Sci., Part A: Polym. Chem.* **31**, 2493 (1993).
- ⁹V. Pryamitsyn and V. Ganesan, *J. Rheol.* **50**, 655 (2006).
- ¹⁰J. Dudowicz, K. F. Freed, and J. F. Douglas, *J. Chem. Phys.* **111**, 7116 (1999).
- ¹¹J. Dudowicz, K. F. Freed, and J. F. Douglas, *J. Chem. Phys.* **112**, 1002 (2000).
- ¹²J. Dudowicz, K. F. Freed, and J. F. Douglas, *J. Chem. Phys.* **113**, 434 (2000).
- ¹³J. Dudowicz, K. F. Freed, and J. F. Douglas, *J. Chem. Phys.* **119**, 12645 (2003).
- ¹⁴R. J. Ellis and A. P. Minton, *Nature (London)* **425**, 27 (2003).
- ¹⁵F. W. Starr and F. Sciortino, *J. Phys.: Condens. Matter* **18**, L347 (2006); J. Largo, F. W. Starr, and F. Sciortino, *Langmuir* **23**, 5896 (2007).
- ¹⁶F. W. Starr, J. F. Douglas, and S. C. Glotzer, *J. Chem. Phys.* **119**, 1777 (2003).
- ¹⁷M. E. Cates and S. J. Candau, *J. Phys.: Condens. Matter* **2**, 6869 (2002).
- ¹⁸J. P. Wittmer, A. Milchev, and M. E. Cates, *J. Chem. Phys.* **109**, 834 (1998).
- ¹⁹M. A. Floriano, E. Caponetti, and A. Z. Panagiotopoulos, *Langmuir* **15**, 3143 (1999); A. Z. Panagiotopoulos, M. A. Floriano, and S. K. Kumar, *Langmuir* **18**, 2940 (2002).
- ²⁰S. Salaniwal, S. K. Kumar, and A. Z. Panagiotopoulos, *Langmuir* **19**, 5164 (2003).
- ²¹E. Bianchi, J. Largo, P. Tartaglia, E. Zaccarelli, and F. Sciortino, *Phys. Rev. Lett.* **97**, 168301 (2006); E. Zaccarelli, I. S. Voivod, S. V. Buldyrev, A. J. Moreno, P. Tartaglia, and F. Sciortino, *J. Chem. Phys.* **124**, 124908 (2006); C. De Michele, S. Gabrielli, P. Tartaglia, and F. Sciortino, *J. Phys. Chem. B* **110**, 8064 (2006).
- ²²V. J. Anderson and H. N. W. Lekkerkerker, *Nature (London)* **416**, 811 (2002); H. N. W. Lekkerkerker, *Physica A* **244**, 227 (1997).
- ²³F. Sciortino, S. Mossa, E. Zaccarelli, and P. Tartaglia, *Phys. Rev. Lett.* **93**, 055701 (2004).
- ²⁴S. Mossa, F. Sciortino, P. Tartaglia, and E. Zaccarelli, *Langmuir* **20**, 10756 (2004).
- ²⁵F. Sciortino, P. Tartaglia, and E. Zaccarelli, *J. Phys. Chem. B* **109**, 21942 (2005).
- ²⁶E. J. Meijer and D. Frenkel, *Phys. Rev. Lett.* **67**, 1110 (1991).
- ²⁷D. Bedrov, M. Pekny, and G. D. Smith, *J. Phys. Chem. B* **102**, 996 (1998).
- ²⁸M. Shen and K. F. Freed, *Biophys. J.* **82**, 1791 (2002); *Proteins* **49**, 439 (2002).
- ²⁹M. P. Allen and D. J. Tildesley, *Computer Simulations of Liquids* (Oxford University Press, Oxford, 1987).
- ³⁰D. Frenkel and B. Smit, *Understanding Molecular Simulation* (Academic, San Diego, 2002).
- ³¹M. E. Tuckerman, B. J. Berne, and G. J. Martyna, *J. Chem. Phys.* **94**, 6811 (1991).
- ³²A. K. Wyczalkowska, Kh. S. Adulkadirova, M. A. Anisimov, and J. V. Sengers, *J. Chem. Phys.* **113**, 4985 (2000); F. D. Di Tolla and M. Ronchetti, *Phys. Rev. E* **48**, 1726 (1993).
- ³³To be more specific, there was no phase separation in Ref. 16 over the temperature range studied. This lowest temperatures studied were determined by the time needed for the system to reach an equilibrium state. As a result, it is possible that phase separation does occur at T below that studied. However, at the higher T studied the pronounced effects of particle clustering are already present.
- ³⁴S. Sastry, E. La Nave, and F. Sciortino, *J. Stat. Mech.: Theory Exp.* **2006**, 12010.
- ³⁵C. De Michele, S. Gabrielli, P. Tartaglia, and F. Sciortino, *J. Phys. Chem. B* **110**, 8064 (2006).
- ³⁶N. B. Wilding, *Phys. Rev. E* **52**, 602 (1995).
- ³⁷A. A. Louis, P. G. Bolhuis, J. P. Hansen, and E. J. Meijer, *Phys. Rev. Lett.* **85**, 2522 (2000).
- ³⁸J. B. Hooper and K. S. Schweizer, *Macromolecules* **38**, 8858 (2005).
- ³⁹E. Rabani and S. A. Egorov, *Nano Lett.* **2**, 69 (2002).
- ⁴⁰L. Zhao, Y. Li, C. Zhong, and J. Mi, *J. Chem. Phys.* **124**, 144913 (2006).
- ⁴¹Q. Zhang and L. A. Archer, *J. Chem. Phys.* **121**, 10814 (2004).
- ⁴²M. Doxastakis, Y. L. Chen, and J. J. Pablo, *J. Chem. Phys.* **123**, 034901 (2005).
- ⁴³J. B. Hooper, K. S. Schweizer, T. G. Desai, R. Koshy, and P. Keblinski, *J. Chem. Phys.* **121**, 6986 (2004).
- ⁴⁴S. P. Obukhov and A. N. Semenov, *Phys. Rev. Lett.* **95**, 038305 (2005).
- ⁴⁵P. G. de Gennes, *Scaling Concepts in Polymer Physics* (Cornell University Press, Ithaca, NY, 1979).
- ⁴⁶S. C. Greer, *Annu. Rev. Phys. Chem.* **53**, 173 (2002).
- ⁴⁷K. Van Workum and J. F. Douglas, *Phys. Rev. E* **71**, 031502 (2005).
- ⁴⁸J. Stambaugh, K. Van Workum, J. F. Douglas, and W. Losert, *Phys. Rev. E* **72**, 031301 (2005).
- ⁴⁹F. Sciortino, E. Bianchi, J. F. Douglas, and P. Tartaglia, *J. Chem. Phys.* **126**, 194903 (2007).
- ⁵⁰M. Wertheim, *J. Stat. Phys.* **35**, 19 (1984); **35**, 35 (1984); **42**, 459 (1986).
- ⁵¹D. Stauffer, *Introduction to Percolation Theory* (Taylor and Francis, Philadelphia, PA, 1994).
- ⁵²S. K. Kumar and J. F. Douglas, *Phys. Rev. Lett.* **87**, 188301 (2001).
- ⁵³F. S. Dainton and K. J. Ivin, *Nature (London)* **162**, 705 (1948).
- ⁵⁴P. Schurtenberger, C. Cavaco, F. Tiberg, and O. Regev, *Langmuir* **12**, 2894 (1996).
- ⁵⁵A. Stradner, H. Sedgwick, F. Cardinaux, W. C. K. Poon, S. U. Egelhaaf, and P. Schurtenberger, *Nature (London)* **432**, 492 (2004).
- ⁵⁶L. S. Pam, L. K. Spell, and J. T. Kindt, *J. Chem. Phys.* **126**, 134906 (2007).
- ⁵⁷J. C. Wheeler, S. J. Kennedy, and P. Pfeuty, *Phys. Rev. Lett.* **45**, 1748 (1980); J. C. Wheeler and P. Pfeuty, *Phys. Rev. A* **24**, 1050 (1981).
- ⁵⁸J. Dudowicz, K. F. Freed, and J. F. Douglas (in preparation).
- ⁵⁹Q. Ying, J. Marecek, and B. Chu, *J. Chem. Phys.* **101**, 2665 (1994).
- ⁶⁰H. N. Ghosh, A. V. Sapre, and J. P. Mittal, *J. Phys. Chem.* **100**, 9439 (1996).
- ⁶¹P. Jonkheijm, P. van der Schoot, A. P. H. J. Schenning, and E. W. Meijer, *Science* **13**, 80 (2006).
- ⁶²S. Harrington, P. H. Poole, F. Sciortino, and H. E. Stanley, *J. Chem. Phys.* **107**, 7443 (1997).